Biosensors and Bioelectronics 23 (2008) 1781–1787

Contents lists available at ScienceDirect

Biosensors and Bioelectronics

journal homepage: www.elsevier.com/locate/bios

Amperometric tyrosinase biosensor based on Fe_3O_4 nanoparticles–chitosan nanocomposite

Shengfu Wang[a,b,**], Yumei Tan[a], Dongming Zhao[a], Guodong Liu[b,*]

[a] Ministry-of-Education Key Laboratory for the Synthesis and Application of Organic Functional Molecules & College of Chemistry and Chemical Engineering, Hubei University, Wuhan 430062, PR China
[b] Department of Chemistry and Molecular Biology, North Dakota State University, Fargo, ND 58105-5516,USA

ARTICLE INFO

Article history:
Received 18 November 2007
Received in revised form 13 February 2008
Accepted 15 February 2008
Available online 23 February 2008

Keywords:
Tyrosinase
Biosensor
Phenolic compounds
Fe_3O_4 magnetic nanoparticles
Chitosan

ABSTRACT

A novel tyrosinase biosensor based on Fe_3O_4 nanoparticles–chitosan nanocomposite has been developed for the detection of phenolic compounds. The large surface area of Fe_3O_4 nanoparticles and the porous morphology of chitosan led to a high loading of enzyme and the entrapped enzyme could retain its bioactivity. The tyrosinase–Fe_3O_4 nanoparticle–chitosan bionanocomposite film was characterized with atomic force microscopy and AC impedance spectra. The prepared biosensor was used to determine phenolic compounds by amperometric detection of the biocatalytically liberated quinone at −0.2 V vs. saturated calomel electrode (SCE). The different parameters, including working potential, pH of supporting electrolyte and temperature that governs the analytical performance of the biosensor have been studied in detail and optimized. The biosensor was applied to detect catechol with a linear range of 8.3×10^{-8} to 7.0×10^{-5} mol L^{-1}, and the detection limit of 2.5×10^{-8} mol L^{-1}. The tyrosinase biosensor exhibits good repeatability and stability. Such new tyrosinase biosensor shows great promise for rapid, simple, and cost-effective analysis of phenolic contaminants in environmental samples. The proposed strategy can be extended for the development of other enzyme-based biosensors.

1. Introduction

Phenolic compounds are important contaminants in medical, food and environmental matrices. In view of their high toxicity, reliable analytical procedures are required for sensitive determination at low level in various matrices. Spectrophotometry and chromatography are the commonly used analytical methods (Poerschmann et al., 1997; Chriswell et al., 1975). These analysis methods have a number of disadvantages that limit their applications primarily to laboratory settings and prohibit their use for rapid analyses under field conditions. Many efforts have been devoted to the development of simple and effective analytical methods for the determination of phenolic compounds. Electrochemical tyrosinase biosensors have been proved to be sensitive and convenient tools for this purpose (Besombes et al., 1995; Takashima and Kaneto, 2004; Védrine et al., 2003). In the presence of oxygen, tyrosinase catalyses the oxidation of phenolic compounds to the corresponding *o*-quinones, which are further electrochemically reduced to *o*-diphenols at low potential (Burestedt et al., 1996).

The key issue in the development of tyrosinase biosensor is the effective immobilization of tyrosinase on the electrode surface. Different approaches, such as polymer entrapment (Dempsey et al., 2004), electropolymerization (Xue and Shen, 2002), sol–gels (Zhang et al., 2003; Wang et al., 2000), self-assembled monolayer (SAM) (Tatsuma and Sato, 2004), and covalent linking (Takashima and Kaneto, 2004) have been widely used to construct tyrosinase biosensors. However, some of these methods are relatively complex, requiring the use of solvents that are unattractive to the environment and result in relatively poor stability and bioactivity of tyrosinase. Therefore, searching for a simple and reliable scheme to immobilize tyrosinase is of considerable interest. In recent years, magnetic nanoparticles as special bimolecular immobilizing carriers are becoming the focus of research. Due to its special properties, magnetic nanoparticles have been used in immunology (Ao et al., 2006) and cell separation processes (Sonti and Bose, 1995). The successful applications of magnetic nanoparticles in the immobilization of bimolecular have also been reported (Tanaka and Matsunaga, 2000; Li et al., 2003). Because its good biocompatibility, strong superparamagnetic, low toxicity, and easy preparation process, magnetic nanoparticles have been used to immobilize enzyme in different matrices (Li et al., 2003; Huang et al., 2003; Reetz et al.,

* Corresponding author. Tel.: +1 701 231 8697; fax: +1 701 231 8831.
** Corresponding author. Tel.: +86 27 50865309; fax: +86 27 88663043.
E-mail addresses: wangsf@hubu.edu.cn (S. Wang), guodong.liu@ndsu.edu (G. Liu).

0956-5663/$ – see front matter © 2008 Elsevier B.V. All rights reserved.
doi:10.1016/j.bios.2008.02.014

1998; Cao et al., 2003). Reetz et al. (1998) reported mechanically stable lipases–Fe_3O_4 nanoparticle–sol–gel biocatalysts by simultaneous entrapment of lipase and nanostructured Fe_3O_4 in hydrophobic sol–gel materials. Cao et al. (2003) reported an electrochemical biosensors utilizing electron transfer in heme proteins immobilized on Fe_3O_4 nanoparticles. On the other hand, the biopolymer chitosan offers excellent characteristics such as biocompatibility, film forming ability, nontoxicity, physiological inertness, and high mechanical strength. Thus, it has been extensively used for the immobilization of enzymes and the construction of biosensors (Chen and Gorski, 2001; Feng et al., 2005; Wei et al., 2002).

In this work, we describe a novel electrochemical tyrosinase biosensor for determining phenolic compounds based on the use of a glassy carbon electrode (GCE) modified with tyrosinase–Fe_3O_4 magnetic nanoparticles–chitosan nanobiocomposite film. The proposed biosensor exhibits fast and sensitive amperometric responses to various phenolic compounds in the absence of any other electron mediators. Parameters such as working potential, pH of supporting electrolyte and temperature that governs the analytical performance of the biosensor were studied and optimized. In addition, the analytical performances of the biosensor with respect to repeatability and stability were also evaluated. The new tyrosinase biosensor shows great promise for rapid, simple, and cost-effective analysis of phenolic contaminants in environmental samples. The proposed strategy can be extended for the development of other enzyme-based biosensors.

2. Experiments

2.1. Reagents

Tyrosinase (EC 1.14.18.1, 3900 U mg^{-1} from mushroom) and chitosan were bought from Sigma–Aldrich (St. Louis, Missouri). Fe_3O_4 magnetic nanoparticles with size of about 30 nm were purchased from Anhui Maanshan Powder Engineering Co. (Anhui, China). All other reagents were of analytical grade and were used as received without further purification. Water used in all the experiments was purified through an ion exchange system with a resistance about 18.0 MΩ cm^{-1} (Nanopure, Barnstead, USA). The supporting electrolyte was 0.1 mol L^{-1} phosphate buffer solution (PBS) prepared with Na_2HPO_4 and KH_2PO_4 and the pH was adjusted with NaOH or H_3PO_4.

2.2. Apparatus

All electrochemical measurements were performed with a model CHI660A electrochemical workstation (CH Instruments, TX, USA) controlled by a personal computer. A conventional three-electrode system equipped with a bare GCE or the prepared tyrosinase–Fe_3O_4 nanoparticle–chitosan–GCE as the working electrode, a saturated calomel electrode (SCE) as the reference electrode, and a platinum wire as the auxiliary electrode, was used for all electrochemical measurements.

The pH values of solutions were determined by using a pHS-25 acidity meter (LIDA Instrument, Shanghai, China). Branson 200 ultrasonic cleaner (Branson Ultrasonics Co., USA) was used for cleaning the electrodes. Atomic force microscopy (AFM) images were obtained from a Nanoscope IIIa atomic force microscopy (Digital Instruments, USA) using tapping mode, with commercially ultrasharpened Si_3N_4 tips.

2.3. Fabrication of tyrosinase–Fe_3O_4 nanoparticle–chitosan biosensor

Before each experiment, the GCE (3 mm diameter) was first polished on chamois leather with 0.05 μm alumina powder and then washed ultrasonically in doubly distilled water, anhydrous ethanol, and water, respectively. After these pretreatments, the cleaned GCE was dried in air. Tyrosinase solution with a concentration of 6.4 mg mL^{-1} was prepared in 0.1 mol L^{-1} PBS (pH 6.5). Chitosan solution with a concentration of 5 mg mL^{-1} was prepared by dissolving 10 mg chitosan in 2.0 mL of 0.1 mol L^{-1} acetic acid. The Fe_3O_4 magnetic nanoparticles suspension (1.7 mg mL^{-1}) was prepared by dispersing Fe_3O_4 nanoparticles in doubly distilled water with ultrasonication for about 2 h. To get the best amperometric responses of the biosensor, the composition of the tyrosinase–Fe_3O_4 nanoparticle–chitosan were optimized. Typically, the Fe_3O_4 nanoparticles, chitosan, and tyrosinase with a volume ratio of 1:1:2 were mixed thoroughly, and 10 μL of this mixture was dropped on the surface of the cleaned GCE. Then the electrode was dried at room temperature. Before experiment, the biosensor was immersed in 0.1 mol L^{-1} PBS (pH 6.5) to wash out the nonimmobilized components from the electrode surface. When not in use, the biosensor was preserved at 4 °C in a dry state.

2.4. Electrochemical measurements

Cyclic voltammetric measurements were performed in an unstirred PBS at a scan rate of 50 mV s^{-1}. Amperometric measurements were performed in a 6-mL electrochemical cell containing a magnetically stirred phosphate buffer supported electrolyte. The desired working potential was applied, and transient currents were allowed to decay to a steady-state value. AC impedance measurements were performed in 0.5 mmol L^{-1} $Fe(CN)_6^{3-/4-}$ containing 0.5 mol L^{-1} KNO_3. The frequency scan range was from 5×10^{-2} to 1×10^5 Hz and the amplitude was 5 mV.

3. Results and discussion

3.1. Characterization of tyrosinase–Fe_3O_4 nanoparticles–chitosan nanobiocomposite

The tyrosinase–Fe_3O_4 nanoparticles–chitosan nanobiocomposite film was first characterized with AFM. Fig. 1 presents the typical AFM images of Fe_3O_4 nanoparticles (a), chitosan film (b), Fe_3O_4 nanoparticle–chitosan (c) and tyrosinase–Fe_3O_4 nanoparticles–chitosan nanobiocomposite (d). One can see that Fe_3O_4 nanoparticles (Fig. 1a) show compact globe shape with the diameter of about 30 nm. Short irregular fibers are observed in the chitosan film (Fig. 1b). In the presence of Fe_3O_4, chitosan–Fe_3O_4 film shows a network-like structure and Fe_3O_4 nanoparticles are regularly dispersed in chitosan film (Fig. 1c). Such network-like structure increases effective surface area of the substrate electrode (here is glassy carbon electrode) to load large amount of tyrosinase, and could effectively prevent the leaking of enzyme molecules from the biosensor. When tyrosinase was entrapped in this network-like film, the aggregates of the enzyme molecules exhibit island-like structures (Fig. 1d), which may facilitate the specific reaction between the substrate and the enzyme, resulting in a good amperometric response of the biosensor (Li et al., 2006).

In the current study, AC impedance was also used to characterize the interface properties of tyrosinase–Fe_3O_4 nanoparticles–chitosan nanobiocomposite biosensor. In AC impedance measurements, the semicircle diameter of impedance equals the electron transfer resistance (R_{et}), which controls the electron transfer kinetics of the redox probe at the electrode interface and is an important parameter. Fig. 2 presents the representative impedance spectrum of the bare GCE (a), chitosan–Fe_3O_4–GCE (b), chitosan–GCE (c), chitosan–Fe_3O_4–tyrosinase–GCE (d) and chitosan–tyrosinase–GCE

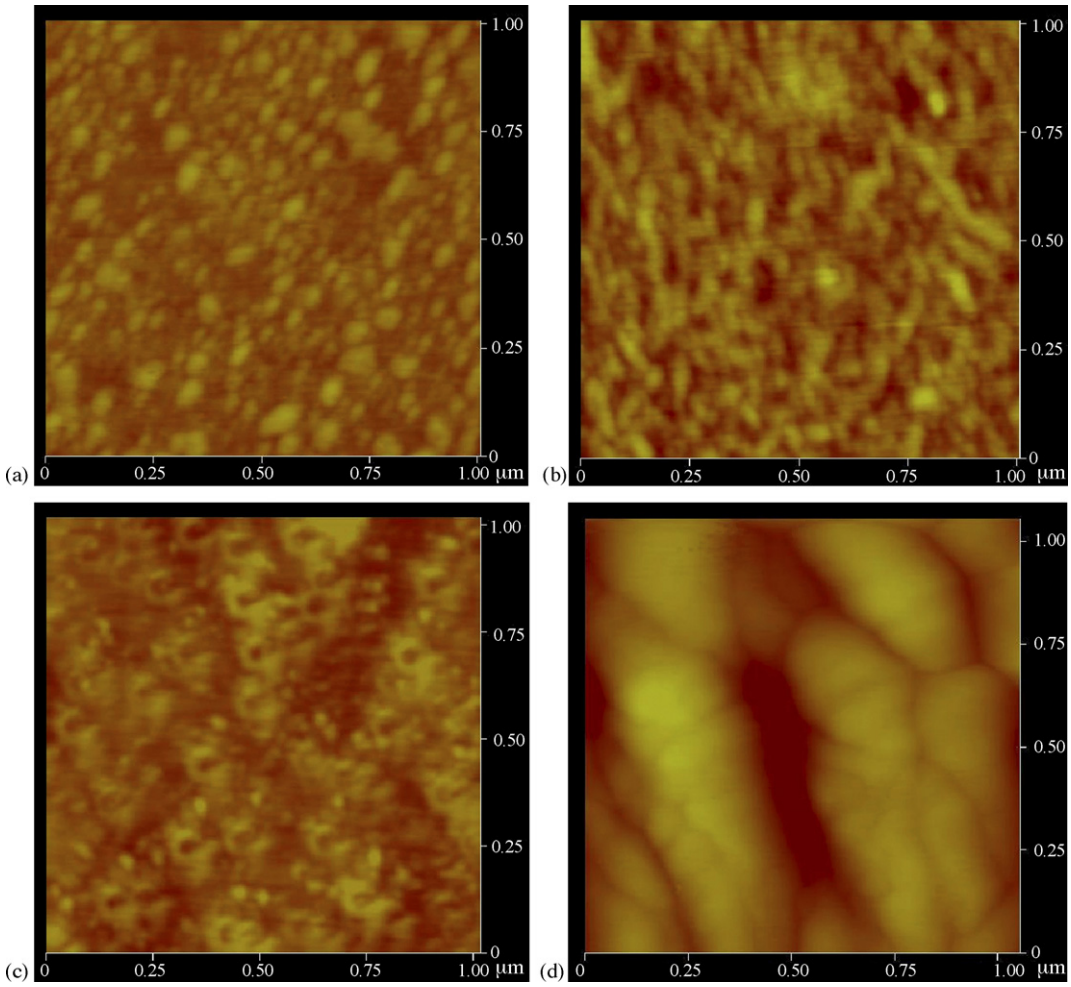

Fig. 1. AFM images of (a) Fe_3O_4, (b) chitosan, (c) chitosan–Fe_3O_4, (d) chitosan–Fe_3O_4–tyrosinase films.

(e) in 0.5 mol L^{-1} KNO_3 solution containing 0.5 mmol L^{-1} $Fe(CN)_6^{3-/4-}$. It can be seen that a straight line was obtained with the bare GCE (curve a) and a well-defined semicircle curve was observed with both the chitosan–Fe_3O_4 nanocomposite film electrode (curve b) and chitosan film electrode (curve c). It indicates the impedance of the electrode increases in the presence of chitosan–Fe_3O_4 nanocomposite and chitosan film, which obstructed the electron transfer of the $Fe(CN)_6^{3-/4-}$. The reason is the non-conductivity of chitosan component in the film. It is noticed that the impedance of chitosan–Fe_3O_4 nanocomposite film is smaller than that of chitosan–GCE. Such decreased impedance may be ascribed to the conductivity of Fe_3O_4 nanoparticles. Lower resistance of the chitosan–Fe_3O_4 nanocomposite film to the electron transfer of the $Fe(CN)_6^{3-/4-}$ is ascribed to the nanosize structure of Fe_3O_4, which could be responsible to proportionates a higher rate of the electron transfer. Moreover, an obvious increase in the interfacial resistance was observed when tyrosinase was entrapped in chitosan–Fe_3O_4 film (curve d). The increase of R_{et} might have been caused by the hindrance of the macromolecular structure of tyrosinase to the electron transfer. On the other hand, the R_{et} of tyrosinase–Fe_3O_4 nanoparticles–chitosan (Fig. 2c) was smaller than that of chitosan–tyrosinase–GCE (curve e), indicating the tyrosinase–Fe_3O_4 nanoparticles–chitosan nanocomposite film allowed greater permeation for $Fe(CN)_6^{3-/4-}$ probe than the pure chitosan film.

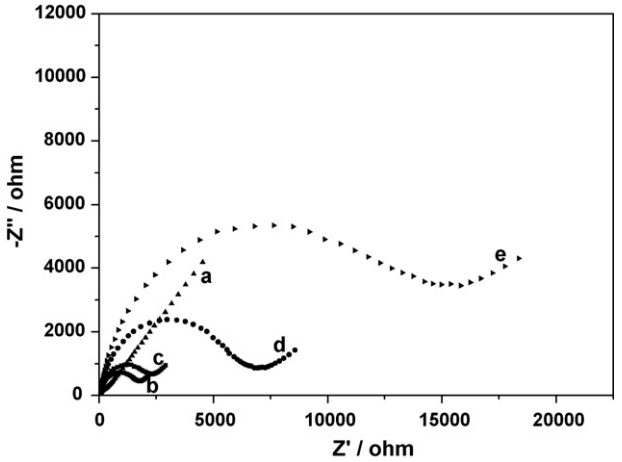

Fig. 2. AC impedance spectrum of (a) the bare GCE, (b) chitosan–Fe_3O_4–GCE, (c) chitosan–GCE, (d) chitosan–Fe_3O_4–tyrosinase–GCE, (e) chitosan–tyrosinase–GCE in 0.5 mmol L^{-1} $Fe(CN)_6^{3-/4-}$ + 0.5 mol L^{-1} KNO_3 solution. The frequency range was from 5×10^{-2} to 1×10^5 Hz.

3.2. Electrochemical sensing characteristics of Fe_3O_4 nanoparticles–chitosan nanobiocomposite biosensor

In current study, catechol was used as phenolic model compound to investigate the electrochemical sensing characteristics

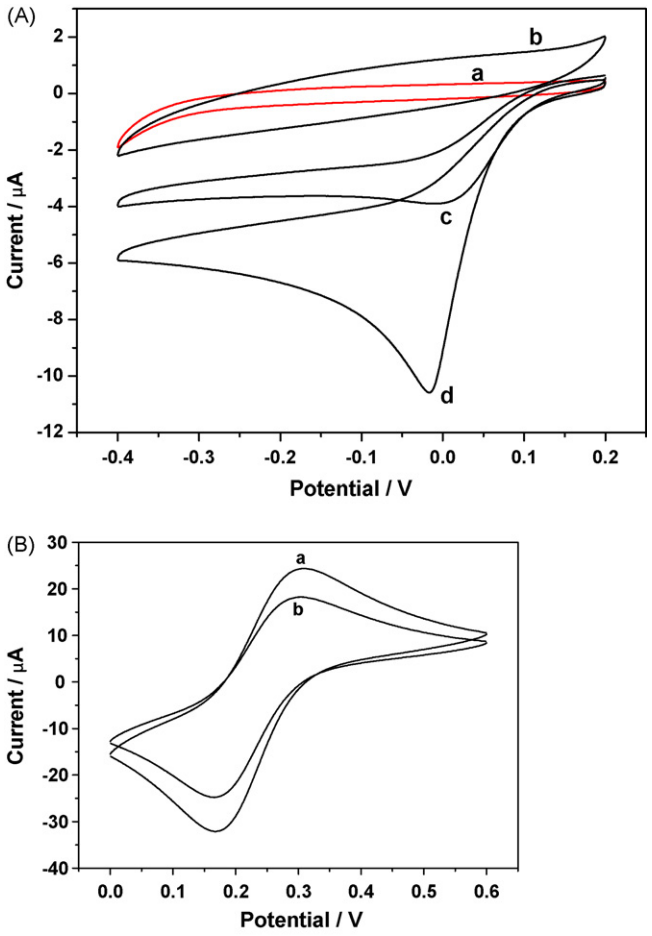

Fig. 3. (A) Cyclic voltammograms of 1.0×10^{-4} mol L^{-1} catechol at (a) GCE; (b) chitosan–Fe_3O_4–GCE; (c) chitosan–tyrosinase–GCE and (d) chitosan–Fe_3O_4–tyrosinase–GCE, Scan rate: 50 mV s^{-1}; supporting electrolyte: 0.1 mol L^{-1} PBS (pH 6.5). (B) Cyclic voltammograms of chitosan–Fe_3O_4–GCE (curve a) and chitosan–GCE (curve b) in 0.5 mmol L^{-1} $Fe(CN)_6^{3-/4-}$ + 0.5 mol L^{-1} KNO_3 solution, potential scan rate: 100 mV s^{-1}.

of the tyrosinase–Fe_3O_4 nanoparticles–chitosan nanobiocomposite biosensor. Fig. 3 shows the typical cyclic voltammograms of catechol at bare GCE (curve a), chitosan–Fe_3O_4–GCE (curve b), tyrosinase–chitosan–GCE (curve c) and tyrosinase–Fe_3O_4 nanoparticles–chitosan (curve d). As expected, there is no redox peak observed at the bare GCE and chitosan–Fe_3O_4–GCE in the absence of tyrosinase even at a concentration of catechol up to 1.0×10^{-4} mol L^{-1}. It indicates that there is no redox activity for catechol in the selected potential range. A well-defined reduction peak at the potential of −0.02 V was observed at the tyrosinase–chitosan–GCE (curve c) and tyrosinase–Fe_3O_4 nanoparticles–chitosan–GCE (curve d). Obviously, the observed reduction peak was attributed to the direct reduction of quinone liberated from the enzyme-catalyzed reaction on the electrode surface. The steps of the enzymatic reaction were shown as follows (Liu et al., 2000):

$$\text{catechol} + \text{tyrosinase}(O_2) \rightarrow o\text{-quinone} + H_2O \quad (1)$$

$$o\text{-quinone} + 2H+ + 2e- \rightarrow \text{catechol}(\text{at electrode}) \quad (2)$$

Comparing the reduction peak currents of catechol at tyrosinase–chitosan–GCE and tyrosinase–Fe_3O_4 nanoparticles–chitosan–GCE, one can see that the Fe_3O_4 nanoparticles in the nanobiocomposite dramatically enhance electrochemical response of catechol, resulting an increasing reduction current. Above results indicate that Fe_3O_4 nanoparticles played an important role in immobilizing tyrosinase and enhancing the enzyme catalytic sites accessible to substrate molecules. To further confirm the role of Fe_3O_4 nanoparticle in the biosensor, cyclic voltammetric experiments with chitosan–GCE and Fe_3O_4 nanoparticle–chitosan–GCE were performed in 0.5 mol L^{-1} KNO_3 solution containing 0.5 mmol L^{-1} $Fe(CN)_6^{3-/4-}$ (Fig. 3(B)). It can be seen that the redox peak currents of $Fe(CN)_6^{3-/4-}$ on the chitosan–Fe_3O_4–GCE is bigger than that on the chitosan–GCE. It indicates the incorporation of Fe_3O_4 in the chitosan film increase its penetrability for $Fe(CN)_6^{3-/4}$, which is consistent with the results of impedance spectrum (see Fig. 2). Additionally, using the proposed tyrosinase–Fe_3O_4 nanoparticles–chitosan, there was no need to use any electron mediators. As reported in the literature (Wang et al., 2002), when the tyrosinase was immobilized on the GCE with chitosan, extra electron mediators such as $Fe(CN)_6^{4-}$ had to be employed.

3.3. Optimization of experimental parameters

The principle of the typical electrochemical tyrosinase biosensor is based on the amperometric detection of the enzymatic product *o*-quinone, which is generated during the course of the tyrosinase-catalyzed oxidation of catechol in the presence of dissolved oxygen. In this work, amperometric measurements were carried out in air-saturated phosphate buffer solution. Although Fig. 3 provides voltammetric information of *o*-quinone on the tyrosinase–Fe_3O_4 nanoparticles–chitosan nanobiocomposite biosensor, it is not accurate to obtain the optimal working potential for the sensitive detection of enzymatic produced *o*-quinone. To determine the optimum potential for the biosensor operation, hydrodynamic voltammetric studies were carried out with 3 μmol L^{-1} catechol. The working electrode was operated at a different potential (between −0.4 and 0 V, 50 mV potential step), and the transient currents were allowed to decay to a steady-state value. Fig. 4(A) displays the effect of the working potential of biosensor on the amperometric response of 3 μmol L^{-1} catechol and the background currents. The reduction current of *o*-quinone was initially observed at 0 V, and it increased rapidly as the applied potential shifted from 0 to −0.4 V, which was due to the increased driving force for the fast reduction of *o*-quinone at low potential. At the same time, background current also increased as the potential became more negative from 0 to −0.4 V. The highest ratio of signal-to-background current was obtained at −0.2 V. When the applied potential was more negative than −0.2 V, a higher signal current was achieved, but the background current also increased distinctly. Moreover, lower potential can bring interferences from electroactive species. Therefore, a working potential of −0.2 V was selected for the future amperometric measurements.

Another parameter affecting the amperometric response of the biosensor is the pH of supporting electrolyte. Fig. 4(B) presents the pH dependence of the amperometric response of 3 μmol L^{-1} catechol in the pH range 4.0–9.0. It can be seen that the response current increases with increasing pH value from 4.0 to 6.5, and then decreases as pH increases further. At low pH, the increase in amperometric response with an increasing pH was attributed to the increase of the enzyme activity. When the pH > 6.5, the decrease of the amperometric response was due to the involvement of protons in the reduction reaction of *o*-quinone. The optimum biosensor response was achieved at pH 6.5, which is consistent with the optimum pH of 6.5 in bulk water (Bru et al., 1989) and the optimum pH range of 5–8 (Xue and Shen, 2002) reported for the free tyrosinase. This indicated that the immobilization procedure had not altered the activity of tyrosinase significantly. Moreover,

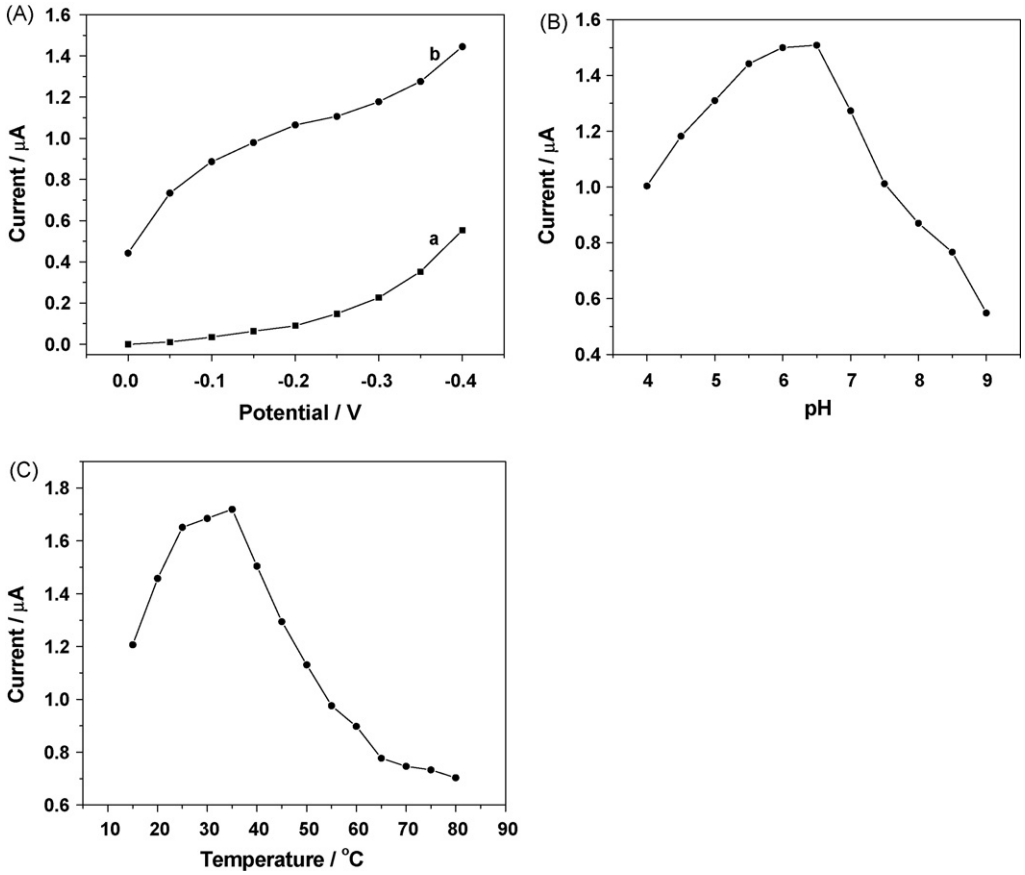

Fig. 4. (A) Effect of working potential on the amperometric response of the biosensor in the absence (curve a) and presence (curve b) of 3 μmol L^{-1} catechol in 0.1 mol L^{-1} PBS (pH 6.5). (B) Effect of pH on the amperometric response of 3 μmol L^{-1} catechol in 0.1 mol L^{-1} PBS. Working potential: −0.2 V vs. SCE. (C) Effect of temperature on the amperometric response of 3 μmol L^{-1} catechol in 0.1 mol L^{-1} PBS (pH 6.5). Working potential: −0.2 V vs. SCE.

the tyrosinase would lose activity irreversibly at lower or higher pH values (Liu et al., 2000). Therefore, a 0.1 mol L^{-1} PBS with pH 6.5 was selected as the supporting electrolyte in the current study.

The effect of temperature on the amperometric response of catechol was also studied. Before amperometric detection, the biosensor was immersed into the buffer solution at a given temperature for 10 min, and then the steady-state current was recorded at this temperature. As can be seen from Fig. 4(C), the response first increases with increasing temperature from 15 to 35 °C, and then decreases sharply as the temperature increases further. Maximum response attains at 35 °C. At higher temperatures, the current response decreases sharply due to the partial denaturation of the tyrosinase. Although the response of the biosensor was greatest at 35 °C, considering most enzymes could be easily denatured at high temperature and the practical applications that require simple experimental procedure and long lifetime of the biosensor, so room temperature was selected throughout the study.

3.4. Analytical performance of the biosensor

The electrochemical biosensing of catechol was performed under the optimized experimental conditions. Fig. 5(A, curve b) displays a typical current–time plot for the tyrosinase–Fe_3O_4 nanoparticles–chitosan on successive additions of 1.0×10^{-3} mol L^{-1} catechol to 0.1 mol L^{-1} PBS (pH 6.5) at an applied potential of −200 mV. Upon an aliquot of catechol was added to the supporting solution, the biosensor responded rapidly to the change of catechol concentration and reached 95% of steady-state current within 2 s, which was faster than that of 1–2 min reported at a tyrosinase–Al_2O_3–sol–gel modified electrode (Liu et al., 2000). Such fast response was attributed to the rapid diffusion of catechol from bulk solution to the immobilized tyrosinase. To compare the analytical performance of chitosan–Fe_3O_4–tyrosinase–GCE with the chitosan–tyrosinase–GCE, the amperometric response of catechol at chitosan–tyrosinase–GCE was studied under the same conditions (Fig. 5A, curve a). Also shown in insets of Fig. 5 are the amperometric responses and corresponding calibration curves of low concentrations of catechol. The corresponding calibration curves of the two modified electrodes in the catechol concentration range from 8.3×10^{-8} to 7.0×10^{-5} mol L^{-1} are shown in Fig. 5(B). The sensitivity and apparent Michaelis–Menten constants (K_M^{app}) of the tyrosinase–Fe_3O_4 nanoparticles–chitosan were 0.514 A (mol L^{-1})$^{-1}$ and 96.9 μmol L^{-1}, respectively (Fig. 5B, curve b). However, the sensitivity and K_M^{app} obtained with the chitosan–tyrosinase–GCE were 0.301 A (mol L^{-1})$^{-1}$ and 167.2 μmol L^{-1}, respectively (Fig. 5B, curve a). The K_M^{app} values were lower than that reported for the free enzyme in solution, which was estimated to be 240 μmol L^{-1} using catechol as the substrate (Smith and Krueger, 1962), 300 μmol L^{-1} using catechol and 700 μmol L^{-1} using phenol as the substrate (Espín et al., 2000). Such low K_M^{app} values may be ascribed to the high concentration of tyrosinase on the biosensor and some electroenzymatic phenomenon. Additionally, the incorporated Fe_3O_4 nanoparticle in the nanobiocomposite may increase the enzyme catalytic sites accessible to substrate molecules.

Table 1
The response characteristics of the biosensor to various phenolic compounds

Phenolic compound	Linear range (mol L^{-1})	Correlation coefficient	Detection limit (mol L^{-1})	Sensitivity (A(mol L^{-1})$^{-1}$)	Relative standard deviation (n = 5)	K_M^{app} (μmol L^{-1})	I_{max} (μA)
Catechol	8.3×10^{-8} to 7.0×10^{-5}	0.999	2.5×10^{-8}	0.514	4.5%	96.9	83.6
p-Cresol	8.3×10^{-8} to 7.8×10^{-5}	0.999	2.5×10^{-8}	0.360	3.2%	130.0	73.4
Phenol	8.3×10^{-8} to 8.3×10^{-5}	0.999	2.5×10^{-8}	0.225	5.0%	159.5	53.9

From above results, one can conclude that the tyrosinase–Fe_3O_4 nanoparticles–chitosan nanobiocomposite biosensor exhibits higher sensitivity than chitosan–tyrosinase–GCE biosensor. Such higher sensitivity may be attributed to the better biocompatible microenvironment and higher permeability provided by the nanobiocomposite film compared to those of the pure chitosan matrix.

3.5. Response characteristics of the biosensor to various phenolic compounds

Three phenolic compounds (catechol, *p*-cresol and phenol) were detected by the tyrosinase–Fe_3O_4 nanoparticles–chitosan–GCE biosensor. The analytical characteristics of the biosensor, including linear range, correlation coefficient, detection limit, sensitivity, K_M^{app} and I_{max} are summarized in Table 1. Compared with the recently reported tyrosinase-modified biosensors on different electrode substrates (Dempsey et al., 2004; Liu et al., 2003; Kaneto, 2005), the linear range of the tyrosinase–Fe_3O_4 nanoparticles–chitosan biosensor was wider and the sensitivity was higher. This behavior might be explained by higher loading of tyrosinase because of an efficient entrapping of enzyme in the nanobiocomposite film, and the decrease of the resistance of the biosensor upon the addition of Fe_3O_4 nanoparticle into the membrane (Fig. 2b). The sensitivity trend was catechol > *p*-cresol > phenol, and this sensitivity order was consistent with the result reported by Fan et al. (2007). The difference in sensitivity might depend on the tyrosinase catalytic selectivity for different phenolic compounds. The K_M^{app} was generally used to evaluate the enzymatic affinity. They were 96.9, 130.0 and 159.5 μmol L^{-1} for catechol, *p*-cresol and phenol, respectively. The K_M^{app} values were lower than that reported for the free enzyme in solution, which was estimated to be 240 μmol L^{-1} using catechol as the substrate (Smith and Krueger, 1962), 300 μmol L^{-1} using catechol and 700 μmol L^{-1} using phenol as the substrate (Espín et al., 2000). The low K_M^{app} values demonstrated that the immobilized tyrosinase possessed high enzymatic activity and exhibited high affinity to phenolic compounds.

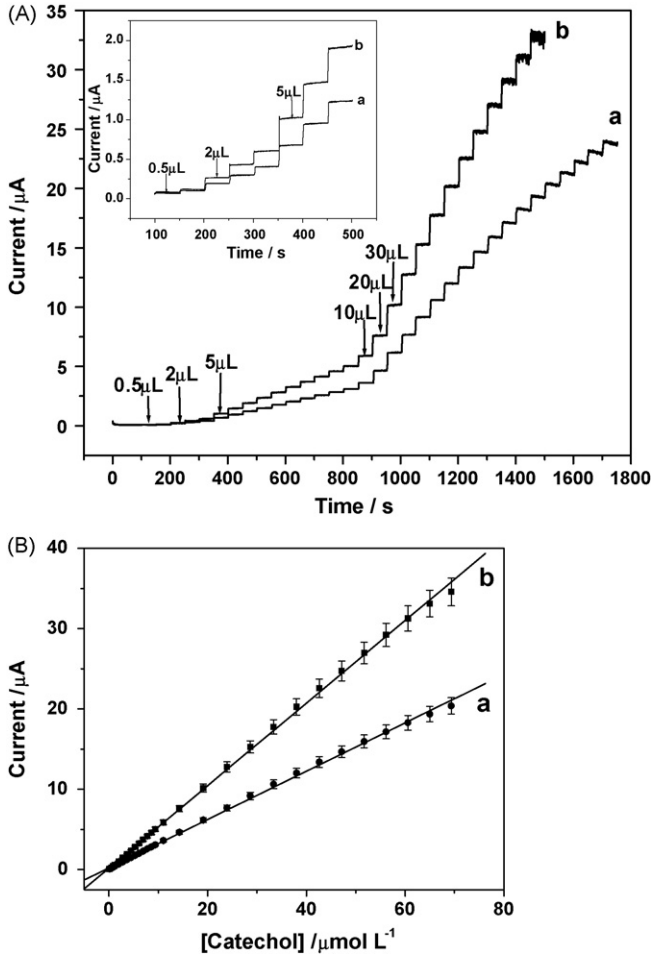

Fig. 5. (A) Typical current–time response curves for the successive addition of 1.0×10^{-3} mol L^{-1} catechol in 0.1 mol L^{-1} PBS (pH 6.5) at (a) chitosan–Fe_3O_4–tyrosinase–GCE and (b) chitosan–tyrosinase–GCE at an applied potential of −0.2 V vs. SCE. Inset: the magnification of the first eight steps. (B) Calibration curves for catechol obtained at (a) chitosan–tyrosinase–GCE and (b) chitosan–Fe_3O_4–tyrosinase–GCE.

3.6. Reproducibility and stability of the biosensor

The repeatability of the same tyrosinase–Fe_3O_4 nanoparticles–chitosan–GCE biosensor was examined by the detection of 5 μmol L^{-1} catechol. A relative standard deviation (R.S.D.) value of 2.7% was obtained for ten successive determinations, which indicated a good repeatability of the measurements with no need to apply a complicated pretreatment procedure to the electrode. The fabrication reproducibility was also estimated with five different electrodes constructed independently by the same procedure. The R.S.D. was 4.5% for the steady-state current to 5 μmol L^{-1} catechol, which demonstrated the reliability of the fabrication procedure.

The long-term stability of the biosensor was evaluated by measuring its response to 5 μmol L^{-1} catechol for 2 months. When not in use, the electrode was stored at 4 °C under dry condition. Its current response was tested every 7 day during the first 1 month. Beyond this period, the experiment was carried out once per 10 days. The biosensor retained about 85% of its original response after 1 month, and decreased gradually to about 53% after 2 months. The relatively good stability of the biosensor may be explained by the fact that the film could provide a biocompatible microenvironment and the specific ability of tyrosinase could be protected effectively.

4. Conclusion

In this work, we have developed a novel tyrosinase biosensor based on the immobilization of tyrosinase in Fe_3O_4 magnetic nanoparticles–chitosan nanobiocomposite for the detection of phenolic compounds. The nanobiocomposite film provided a suitable microenvironment, which could effectively present large loading amount of enzyme and prevent the leaching of the immobilized enzyme. The resulting biosensor exhibited a good analytical performance for the amperometric detection of phenolic com-

pounds without extra mediators, and showed high sensitivity, low detection limit, and good reproducibility. The proposed strategy can be extended for the development of other enzyme-based biosensors.

Acknowledgements

S. Wang acknowledges the financial support from the National Natural Science Foundation of China (No. 20575017) and the Natural Science Foundation of Hubei province (No. 2005ABA063). G. Liu acknowledges the financial support from North Dakota Experimental Program to Stimulate Competitive Research (EPSCoR) and new faculty startup funds of North Dakota State University.

References

Ao, L., Gao, F., Pan, B., He, R., Cui, D., 2006. Anal. Chem. 78, 1104–1106.
Besombes, J.L., Cosnier, S., Labbé, P., Reverdy, G., 1995. Anal. Chim. Acta 311, 255–263.
Bru, R., Sanchez-Ferrer, A., García-Carmona, F., 1989. Biotechnol. Bioeng. 34, 304–308.
Burestedt, E., Narvaez, A., Ruzgas, T., Gorton, L., Emnéus, J., Domínguez, E., Marko-Varga, G., 1996. Anal. Chem. 68, 1605–1611.
Cao, D., He, P., Hu, N., 2003. Analyst 128, 1268–1274.
Chen, L., Gorski, W., 2001. Anal. Chem. 73, 2862–2868.
Chriswell, C.D., Chang, R.C., Fritz, J.S., 1975. Anal. Chem. 47, 1325–1329.
Dempsey, E., Diamond, D., Collier, A., 2004. Biosens. Bioelectron. 20, 367–377.
Espín, J.C., Varón, R., Fenoll, L.G., Gilabert, M.A., García-Ruíz, P.A., Tudele, J., García-Cánovas, F., 2000. Eur. J. Biochem. 267, 1270–1279.
Fan, Q., Shan, D., Xue, H., He, Y., Cosnier, S., 2007. Biosens. Bioelectron. 22, 816–821.
Feng, J.J., Zhao, G., Xu, J.J., Chen, H.Y., 2005. Anal. Biochem. 342, 280–286.
Huang, S.H., Liao, M.H., Chen, D.H., 2003. Biotechnol. Prog. 19, 1095–1100.
Kaneto, R.K., 2005. Curr. Appl. Phys. 5, 178–183.
Li, J., He, X., Wu, Z., Wang, K., Shen, G., Yu, R., 2003. Anal. Chim. Acta 481, 191–198.
Li, Y.F., Liu, Z.M., Liu, Y.L., Yang, Y.H., Shen, G.L., Yu, R.Q., 2006. Anal. Biochem. 349, 33–40.
Liu, S., Yu, J., Ju, H., 2003. J. Electroanal. Chem. 540, 61–67.
Liu, Z., Liu, B., Kong, J., Deng, J., 2000. Anal. Chem. 72, 4707–4712.
Poerschmann, J., Zhang, Z., Kopinke, F.D., Pawliszyn, J., 1997. Anal. Chem. 69, 597–600.
Reetz, M.T., Zonta, A., Vijayakrishnan, V., Schimossek, K., 1998. J. Mol. Catal. A: Chem. 134, 251–258.
Smith, J.L., Krueger, R.C., 1962. J. Biol. Chem. 237, 1121–1128.
Sonti, S.V., Bose, A., 1995. J. Colloid Interf. Sci. 170, 575–585.
Takashima, R.W., Kaneto, K., 2004. Sens. Actuators B 102, 271–277.
Tanaka, T., Matsunaga, T., 2000. Anal. Chem. 72, 3518–3522.
Tatsuma, T., Sato, T., 2004. J. Electroanal. Chem. 572, 15–19.
Védrine, C., Fabiano, S., Tran-Minh, C., 2003. Talanta 59, 535–544.
Wang, B., Zhang, J., Dong, S., 2000. Biosens. Bioelectron. 15, 397–402.
Wang, G., Xu, J.J., Ye, L.H., Zhu, J.J., Chen, H.Y., 2002. Bioelectrochemistry 57, 33–38.
Wei, X., Cruz, J., Gorski, W., 2002. Anal. Chem. 74, 5039–5046.
Xue, H., Shen, Z., 2002. Talanta 57, 289–295.
Zhang, T., Tian, B., Kong, J., Yang, P., Liu, B., 2003. Anal. Chim. Acta 489, 199–206.